Atmos. Chem. Phys. Discuss., 15, 18365–18405, 2015
www.atmos-chem-phys-discuss.net/15/18365/2015/
doi:10.5194/acpd-15-18365-2015

Atmospheric Chemistry and Physics Discussions

Quantifying atmospheric nitrogen deposition through a nationwide monitoring network across China

W. Xu[1], X. S. Luo[1,2], Y. P. Pan[3], L. Zhang[4], A. H. Tang[1], J. L. Shen[5], Y. Zhang[6], K. H. Li[7], Q. H. Wu[1], D. W. Yang[1], Y. Y. Zhang[1], J. Xue[1], W. Q. Li[8], Q. Q. Li[1,9], L. Tang[9], S. H. Lu[10], T. Liang[11], Y. A. Tong[11], P. Liu[12], Q. Zhang[12], Z. Q. Xiong[13], X. J. Shi[14], L. H. Wu[15], W. Q. Shi[16], K. Tian[17], X. H. Zhong[17], K. Shi[18], Q. Y. Tang[19], L. J. Zhang[20], J. L. Huang[21], C. E. He[22], F. H. Kuang[23], B. Zhu[23], H. Liu[24], X. Jin[25], Y. J. Xin[25], X. K. Shi[26], E. Z. Du[27], A. J. Dore[28], S. Tang[28], J. L. Collett Jr.[29], K. Goulding[30], F. S. Zhang[1], and X. J. Liu[1]

[1]College of Resources and Environmental Sciences, China Agricultural University, Beijing 100193, China
[2]Institute of Plant Nutrition, Resources and Environmental Sciences, Henan Academy of Agricultural Sciences, Zhengzhou 450002, China
[3]State Key Laboratory of Atmospheric Boundary Layer Physics and Atmospheric Chemistry (LAPC), Institute of Atmospheric Physics, Chinese Academy of Sciences, Beijing 100029, China

[4]Laboratory for Climate and Ocean-Atmosphere Studies, Department of Atmospheric and Oceanic Sciences, School of Physics, Peking University, Beijing 100871, China
[5]Institute of Subtropical Agriculture, Chinese Academy of Sciences, Changsha 4410125, China
[6]College of Nature Conservation, Beijing Forestry University, Beijing 100083, China
[7]Xinjiang Institute of Ecology and Geography, Chinese Academy of Sciences, Urumqi 830011, China
[8]Fujian Institute of Tobacco Agricultural Sciences, Fuzhou 350003, China
[9]College of Resources and Environmental Sciences, Yunnan Agricultural University, Kunming 650224, China
[10]Soil and Fertilizer Institute, Sichuan Academy of Agricultural Sciences, Chengdu 610066, China
[11]Nature Resource and Environment College, Northwest A&F University, Yangling 712100, China
[12]Institute of Agricultural Environment and Resource, Shanxi Academy of Agricultural Sciences, Taiyuan 030031, China
[13]College of Resources and Environmental Sciences, Nanjing Agricultural University, Nanjing 210009, China
[14]College of Resources and Environment, Southwest University, Chongqing 400716, China
[15]College of Environmental and Resource Sciences, Zhejiang University, Hangzhou 310029, China
[16]South Subtropical Crops Research Institute, Chinese Academy of Tropical Agricultural Science, Zhanjiang 524091, China
[17]Rice Research Institute, Guangdong Academy of Agricultural Sciences, Guangzhou 510640, China
[18]College of Environmental and Chemical Engineering, Dalian Jiaotong University, Dalian 116028, China
[19]College of Agriculture, Hunan Agricultural University, Changsha 410128, China
[20]College of Resources and Environment, Agricultural University of Hebei, Baoding 071001, China
[21]College of Plant Science and Technology, Huazhong Agricultural University, Wuhan, China

ACPD
15, 18365–18405, 2015

[22]Institute of Geographic Sciences and Natural Resources, Chinese Academy of Sciences, Beijing 100101, China
[23]Institute of Mountain, Hazards and Environment, Chinese Academy of Sciences, Chengdu 610041, China
[24]Research Institute of Soil & Fertilizer and Agricultural Water Conservation, Xinjiang Academy of Agricultural Sciences, Urumqi 830091, China
[25]The Bureau of Qinghai Meteorology, Xining 810001, China
[26]Agriculture, Forestry and Water Department of Changdao County, Changdao 265800, China
[27]State Key Laboratory of Earth Surface Processes and Resource Ecology, and College of Resources Science & Technology, Beijing Normal University, Beijing 100875, China
[28]Centre for Ecology & Hydrology Edinburgh, Bush Estate, Penicuik, Midlothian EH26 0QB, UK
[29]Department of Atmospheric Science, Colorado State University, Fort Collins, CO 80523, USA
[30]The Sustainable Soils and Grassland Systems Department, Rothamsted Research, Harpenden AL5 2JQ, UK

Received: 17 June 2015 – Accepted: 19 June 2015 – Published: 07 July 2015

Correspondence to: X. J. Liu (liu310@cau.edu.cn)

Published by Copernicus Publications on behalf of the European Geosciences Union.

ACPD
15, 18365–18405, 2015

Abstract

Global reactive nitrogen (N_r) deposition to terrestrial ecosystems has increased dramatically since the industrial revolution. This is especially true in recent decades in China due to continuous economic growth. However, there are no comprehensive reports of both measured dry and wet N_r deposition across China. We therefore conducted a multiple-year study during the period mainly from 2010 to 2014 to monitor atmospheric concentrations of five major N_r species of gaseous NH_3, NO_2 and HNO_3, and inorganic nitrogen (NH_4^+ and NO_3^-) in both particles and precipitation, based on a Nationwide Nitrogen Deposition Monitoring Network (NNDMN, covering 43 sites) in China. Wet deposition fluxes of N_r species were measured directly; dry deposition fluxes were estimated using airborne concentration measurements and inferential models. Our observations reveal large spatial variations of atmospheric N_r concentrations and dry and wet N_r deposition. The annual average concentrations (1.3–47.0 μg N m^{-3}) and dry plus wet deposition fluxes (2.9–75.2 kg N ha^{-1} yr^{-1}) of inorganic N_r species ranked by region as North China > Southeast China > Southwest China > Northeast China > Northwest China > the Tibetan Plateau or by land use as urban > rural > background sites, reflecting the impact of anthropogenic N_r emission. Average dry and wet N deposition fluxes were 18.5 and 19.3 kg N ha^{-1} yr^{-1}, respectively, across China, with reduced N deposition dominating both dry and wet deposition. Our results suggest atmospheric dry N deposition is equally important to wet N deposition at the national scale and both deposition forms should be included when considering the impacts of N deposition on environment and ecosystem health.

1 Introduction

Humans continue to accelerate the global nitrogen (N) cycle at a record pace as rates of anthropogenic reactive nitrogen (N_r) fixation have increased 20-fold over the last century (Galloway et al., 2008). New N_r from anthropogenic fixation is formed primar-

ACPD
15, 18365–18405, 2015

ily through cultivation of N-fixing legumes, the Haber–Bosch process and combustion of fossil-fuel (Galloway et al., 2013). As more N_r have been created, emissions of N_r ($NO_x = NO + NO_2$, and NH_3) to the atmosphere have increased from approximately 34 Tg N yr^{-1} in 1860 to 109 Tg N yr^{-1} in 2010 (Fowler et al., 2013; Galloway et al., 2004); most of this emitted N_r is deposited back to land and water bodies. As an essential nutrient, N supplied by atmospheric deposition is useful for all life forms in the biosphere and may stimulate primary production in an ecosystem if it does not exceed the ecosystem-dependent critical load (Liu et al., 2010, 2011). However, long-term high levels of atmospheric N_r and its deposition can reduce biological diversity (Clark et al., 2008), degrade human health (Richter et al., 2005), alter soil and water chemistry (Vitousek et al., 1997) and influence the greenhouse gas balance (Matson et al., 2002).

Nitrogen deposition occurs via dry and wet processes. Neglecting dry deposition can lead to substantial underestimation of total flux as dry deposition can contribute up to 2/3 of total N deposition (Flechard et al., 2011). For quantification of atmospheric deposition at the national scale, long-term monitoring networks such as CASTNET/NADP (the United States), EMEP (Europe) and EANET (East Asia) have been established globally; such networks are essential for quantification of both wet and dry deposition and revealing long-term trends and spatial patterns under major environmental and climate change (Skeffington and Hill, 2012). Wet deposition, by means of rain or snow, is relatively easily measured in existing networks. In contrast, dry deposition of gases and particulate matter is much more difficult to measure, and strongly influenced by factors such as surface roughness, surface wetness, and climate and environmental factors (Erisman et al., 2005). Direct methods (e.g., eddy correlation, chambers) and indirect methods (e.g., inferential, gradient analysis) can determine dry deposition fluxes (Seinfeld and Pandis, 2006). The inferential method is widely used in many monitoring networks (e.g. CASTNET, EMEP and EANET), where dry deposition rates are derived from measured ambient concentrations of N_r species and computed deposition velocities (Endo et al., 2011; Holland et al., 2005; Pan et al., 2012). Additionally, atmospheric

ACPD
15, 18365–18405, 2015

modeling has been used as an operational tool to upscale results from sites to regions where no measurements are available (Flechard et al., 2011; Zhao et al., 2015).

According to long-term trends observed by the above monitoring networks, N deposition has decreased over the last two decades in Europe (EEA, 2011). Measurements of wet deposition in the US show a strong decrease in NO_3-N deposition over most of the country (Du et al., 2014), but NH_4-N deposition increased in agricultural regions. China, as one of the most rapidly developing countries in East Asia, has witnessed serious atmospheric N_r pollution since the late 1970s (Hu et al., 2010; Liu et al., 2011). Accurate quantification of N deposition is key to assessing its ecological impacts on terrestrial ecosystems (Liu et al., 2011). Previous modeling studies (e.g., Dentener et al., 2006; Galloway et al., 2008) suggested that central-east China was a global hotspot for N deposition. More recently, based on meta-analyses of historic literature, both Liu et al. (2013) and Jia et al. (2014) reported a significant increase in N wet/bulk deposition in China since the 1980s or 1990s. However, most measurements in China only reported wet/bulk deposition (e.g., Chen et al., 2007; Huang et al., 2013; Zhu et al., 2015) and/or dry deposition (Luo et al., 2013; Shen et al., 2009; Pan et al., 2012) at a local or regional scale. Although national N deposition has been investigated by Lü and Tian (2007, 2014), the deposition fluxes were largely underestimated due to the inclusion only of gaseous NO_2 in dry deposition and not NH_3, HNO_3 and particulate ammonium and nitrate etc. Therefore, the magnitude and spatial patterns of in situ measured N wet and dry deposition across China are still not clear.

Against such a background, we have established a Nationwide Nitrogen Deposition Monitoring Network (NNDMN) in China in 2010, measuring both wet and dry deposition. The NNDMN consists of forty-three in situ monitoring sites, covering urban, rural (cropland) and background (coastal, forest and grassland) areas across China. The focus of the network is to conduct high-quality measurements of atmospheric N_r in gases, particles and precipitation. These data provide a unique and valuable quantitative description of N_r deposition in China, but have never been published as a whole. The objectives of this study were therefore to: (1) obtain the first quantitative infor-

ACPD
15, 18365–18405, 2015

mation on atmospheric N_r concentrations and pollution status across China; and (2) analyze overall fluxes and spatial variations of N wet and dry deposition in relation to anthropogenic N_r emissions in different regions.

2 Materials and methods

2.1 Sampling sites

The distribution of the forty-three monitoring sites in the NNDMN is shown in Fig. 1. Although sampling periods varied between sites, most of our monitoring started from 2010 to 2014 (see Supporting Materials for details). The NNDMN comprise 10 urban sites, 22 rural sites and 11 background sites (Table S1 of the Supplement). To better analyze atmospheric N deposition results among the sites, we divided the forty-three sites into six regions: north China (NC, 13 sites), northeast China (NE, 5 sites); northwest China (NW, 6 sites), southeast China (SE, 11 sites), southwest China (SW, 6 sites), and Tibetan Plateau (TP, 2 sites), representing China's various social-economical and geo-climatic regions (for details, see Sect. S1 of the Supplement). The sites in the six regions are described using region codes (i.e., NC, NE, NW, SE, SW, TP) plus site numbers such as NC1, NC2, NC3, . . . , NE1, NE2, etc. The longitudes and latitudes of all 43 sites ranged from 83.71 to 129.25° E, and from 21.26 to 50.78° N, respectively. Annual mean rainfall ranged from 170 to 1748 mm and the annual mean air temperature ranged from −6.2 to 23.2 °C. Site names, land use types and population densities are summarized in Table S1. More detailed information on the monitoring sites, such as specific locations, surrounding environment and possible emission sources are provided in Sect. S2 of the Supplement.

2.2 Collection of gaseous and particulate N_r samples

In this study ambient N_r concentrations of gaseous NH_3, NO_2 and HNO_3, and particulate NH_4^+ (pNH_4^+) and NO_3^- (pNO_3^-) were measured monthly at the 43 sites using

ACPD
15, 18365–18405, 2015

continuous active and passive samplers. DELTA active sampling systems (DEnuder for Long-Term Atmospheric sampling, described in detail in Flechard et al. (2011) and Sutton et al. (2001), were used to collect NH_3, HNO_3, pNH_4^+ and pNO_3^-; NO_2 samples were collected using Gradko diffusion tubes (Gradko International Limited, UK). The air intakes of the DELTA system and the NO_2 tubes were set at a height of 2 m above the ground (at least 0.5 m higher than the canopy height) at most sites. At a few sites, the DELTA systems could not be used due to power constraints. Therefore, NH_3 and NO_2 samples were collected using ALPHA passive samplers (Adapted Low-cost High Absorption, designed by the Center for Ecology and Hydrology, Edinburgh, UK) and Gradko diffusion tubes, respectively, while the pNH_4^+ and pNO_3^- in PM_{10} were collected using particulate samplers (TSH-16 or TH-150III, produced by Wuhan Tianhong Corp., Wuhan, China). Briefly, all the measurements of N_r concentration were based on monthly sampling (one sample per month for each N_r species) except at the very few sites without DELTA systems, where pNH_4^+ and pNO_3^- samples were calculated from daily sampling transformed to monthly averaged data. Detailed information on measuring methods, sample replication and collection are given in Sect. S3 of the Supplement with sampling periods listed in Table S2 of the Supplement. Comparisons between the ALPHA samplers and the DELTA systems at six network sites for gaseous NH_3 measurements indicated that the two methods provided comparable NH_3 concentrations (values between the two methods were not significantly different) (cf. Sect. S4 in the Supplement and Fig. S1 therein).

2.3 Collection of precipitation

At all monitoring sites precipitation samples were collected using precipitation gauges (SDM6, Tianjin Weather Equipment Inc., China) located beside the DELTA systems (ca. 2 m). The collector, consisting of a stainless steel funnel and glass bottle (vol. 2000–2500 mL), collects precipitation (rainwater, snow) without a power supply. Precipitation was measured using a graduated cylinder (scale range: 0–10 mm; division: 0.1 mm) coupled with the gauge. After each daily (8:00 a.m.–8:00 a.m. next day) event,

ACPD
15, 18365–18405, 2015

the collected samples were thoroughly mixed and then immediately stored in clean polyethylene bottles (50 mL). All collected samples (including melted snow) samples were frozen at −18 °C at each site until delivery to the laboratory at China Agricultural University (CAU) for analysis of inorganic N (NH_4^+ and NO_3^-). The gauges were cleaned with high-purity water after each collection and once every week in order to avoid cross contamination.

2.4 Analytical procedures

In CAU's analytical laboratory, the exposed sampling trains of the DELTA systems and passive samples were stored at 4 °C and analyzed at one-month intervals. The HNO_3 denuders and alkaline-coated filters were extracted with 10 mL 0.05 % H_2O_2 in aqueous solution. The NH_3 denuders and acid-coated filters, and ALPHA samplers were extracted with 10 mL high-purity water. The loaded PM_{10} filters were extracted with 50 mL high-purity water by ultrasonication for 30–60 min and then filtered through a syringe filter (0.45 µm, Tengda Inc., Tianjin, China). Ammonium (NH_4^+) and nitrate (NO_3^-) in the extracted and filtered solutions were measured with an AA3 continuous-flow analyzer (Bran + Luebbe GmbH, Norderstedt, Germany). The detection limits were 0.01 mg N L^{-1} for NH_4^+ and NO_3^-. It should be noted that NO_3^- was converted to NO_2^- during the chemical analysis. So, NO_2^- here was included in the analysis, and NO_3^- equals to the sum of NO_2^- and NO_3^-. The disks from the Gradko samplers were extracted with a solution containing sulphanilamide, H_3PO_4 and N-1-Naphthylethylenediamine, and the NO_2^- content in the extract determined using a colorimetric method by absorbance at a wavelength of 542 nm. The detection limit for NO_2^- was 0.01 mg N L^{-1}. Three laboratory and three field blank samples were extracted and analyzed using the same methods as the exposed samples. After correcting for the corresponding blanks, the results were used for the calculation of ambient concentrations of gaseous and particulate N_r. Each collected precipitation sample was filtered with a 0.45 µm syringe filter, and 15 mL filtrates frozen and stored in polypropylene bottles until chemical analysis

ACPD
15, 18365–18405, 2015

within one month. The NH_4^+ and NO_3^- concentrations of the filtrates were determined using an AA3 continuous-flow analyzer as described above.

2.5 Deposition flux estimation

The inferential technique, which combines the measured concentration and a modeled dry deposition velocity (V_d), was used to estimate the dry deposition fluxes of N_r species (Schwede et al., 2011; Pan et al., 2012). The concentrations of gases (HNO_3, NO_2 and NH_3) and aerosols (NH_4^+ and NO_3^-) were measured as described in Sect. 2.2. The monthly average V_d over China was calculated by the GEOS-Chem chemical transport model (CTM) (Bey et al., 2001; http://geos-chem.org). The GEOS-Chem CTM is driven by GEOS-5 (Goddard Earth Observing System) assimilated meteorological data from the NASA Global Modeling and Assimilation Office (GMAO) with a horizontal resolution of 1/2° latitude × 2/3° longitude and 6 h temporal resolution (3 h for surface variables and mixing depths). We used a nested-grid version of GEOS-Chem for Asia that has the native 1/2° × 2/3° resolution over East Asia (70–150° E, 11° S–55° N) (Chen et al., 2009). The nested model has been applied to examine atmospheric nitrogen deposition to the northwestern Pacific (Zhao et al., 2015), and a similar nested model for North America has been used to analyze nitrogen deposition over the United States (Zhang et al., 2012a; Ellis et al., 2013). The model calculation of dry deposition of N_r species follows a standard big-leaf resistance-in-series model (Wesely, 1989). For a detailed description of the V_d calculation as well as the estimation of N dry deposition, the reader is referred to the Supplement (Sect. S5), with monthly and annual dry deposition velocities of N_r for different land use types presented in Tables S3 and S4 therein.

Wet N deposition flux was calculated as the product of the precipitation amount and the concentration of N_r species in precipitation, using the following Eqs. (1) and (2):

$$C_w = \sum_{i=1}^{n} (C_i P_i) / \sum_{i=1}^{n} P_i \quad (1)$$

ACPD
15, 18365–18405, 2015

where C_w is the volume-weighted mean (VWM) concentration (mg N L^{-1}) calculated from the n precipitation samples within a month or a year, and the individual sample concentration C_i is weighted by the rainfall amount P_i for each sample.

$$D_w = P_t C_w / 100 \quad (2)$$

where D_w is the wet-deposition flux (kg N ha^{-1}), P_t is the total amount of all precipitation events (mm), and 100 is a unit conversion factor.

2.6 Statistics

A one-way analysis of variance (ANOVA) and nonparametric t-tests were conducted to examine the differences in the investigated variables between sites (urban, rural and background) and between the six regions. Linear regression analysis was used to analyze the relationships among annual wet N deposition flux, annual precipitation amount and annual VWM concentration of inorganic N in precipitation. All analyses were performed using SPSS 11.5 (SPSS Inc., Chicago, IL, USA). Statistically significant differences were set at P values < 0.05.

3 Results

3.1 Concentrations of N_r species in air

Monthly mean concentrations of NH_3, NO_2, HNO_3, pNH_4^+ and pNO_3^- were 0.08–34.8, 0.13–33.4, 0.02–4.90, 0.02–55.0 and 0.02–32.1 μg N m^{-3}, respectively (Fig. S2a–e in the Supplement). The annual mean concentrations of gaseous and particulate N_r were calculated for each site from the monthly N_r concentrations (Fig. 2a), and further were averaged over region and land use (Fig. 3a) according to geographical location and the classification of each site as listed in Table 1. Annual mean NH_3 concentrations ranged from 0.3 to 13.1 μg N m^{-3}, with an overall average value of 6.1 μg N m^{-3}.

ACPD
15, 18365–18405, 2015

Among the six regions, the gaseous NH_3 concentrations decreased in the order of NC > SW > NW > SE > NE > TP. In NC, SE and SW, the NH_3 concentrations at the urban sites (average three regions, 9.5 μg N m^{-3}) were slightly higher than at the rural sites (6.2 μg N m^{-3}). The annual mean NH_3 concentration across northern rural sites, on average, was 1.8 times greater than the average of southern rural sites. Annual mean NO_2 concentrations showed similar spatial variations (0.4 to 16.2 μg N m^{-3}) to those of NH_3, and overall averaged 6.8 μg N m^{-3}. The highest NO_2 concentrations were found in NC, with an average value of 10.1 μg N m^{-3}, 1.5–3.6 times greater than the averages of the other five regions. Both the urban and rural sites in NC had relatively high NO_2 concentrations (on average, 13.9 vs. 9.7 μg N m^{-3}). Annual mean HNO_3 concentrations were relatively low everywhere (from 0.1 to 2.9 μg N m^{-3}, averaging 1.3 μg N m^{-3}) and ranked by order of NC > NW ≈ SW > SE > NE. The HNO_3 concentrations were comparable for the same land use types in northern and southern China, on average, 1.8 vs. 1.8, 1.2 vs. 1.0, and 0.6 vs. 0.8 μg N m^{-3} at the urban, rural and background sites, respectively. The annual mean concentrations of pNH_4^+ and pNO_3^- were in the ranges of 0.2–18.0 μg N m^{-3} (average 5.7 μg N m^{-3}) and 0.2–7.7 μg N m^{-3} (average 2.7 μg N m^{-3}), respectively. The regional variation of annual pNH_4^+ concentrations was consistent with that of NH_3, whereas annual pNO_3^- concentrations followed the order: NC > SE > SW > NE ≈ NW > TP. Annual mean concentrations of pNH_4^+ and pNO_3^- at all land use types were both slightly higher in the northern China, compared with those in the other three regions.

In total, annual mean concentrations of gaseous and particulate N_r in air were 1.3–47.0 μg N m^{-3} among all sampling sites; ranked in the order of NC > NW ≈ SW > SE > NE > TP. Comparing land use types, the total annual concentrations of measured N_r, as well as each N_r species, generally decreased in the order of urban > rural > background (Fig. S3).

ACPD
15, 18365–18405, 2015

3.2 Concentrations of N_r species in precipitation

The monthly VWM concentrations of inorganic N_r species at the forty-three sampling sites during the study period ranged from 0.01 to 27.1 mg N L^{-1} for NH_4^+-N and from 0.02 to 27.9 mg N L^{-1} for NO_3^--N (Fig. S4). The regional variations in NH_4^+-N and NO_3^--N were not totally consistent with ambient gaseous and particulate N_r (Figs. S2 and S4). For example, monthly mean concentrations of NH_3 and pNH_4^+ were significantly higher (both $p < 0.05$) in NC than NW, whereas the opposite was observed for precipitation NH_4^+-N. In addition, monthly mean pNO_3^- concentrations were significantly lower ($p < 0.05$) in NE than SE, but significantly higher precipitation NO_3^--N concentrations were found in NE. The annual VWM concentrations of NH_4^+-N and NO_3^--N across all sites were in the ranges of 0.2–4.3 and 0.1–2.5 mg N L^{-1}, respectively, with averages of 1.6 and 1.3 mg N L^{-1} (Fig. 2b) and showing no significant difference ($p > 0.05$) between them. Among regions, annual VWM concentrations ranked in the order of NW > NC > NE ≈ SW ≈ TP > SE for NH_4^+-N, whereas the order was NC > NW > NE > SW > SE > TP for NO_3^--N (Table 1). Annual total inorganic N concentrations in precipitation averaged 4.3, 2.3, 3.9 and 2.0 mg N L^{-1} in NC, NE, NW and SW respectively, and 1.9 mg N L^{-1} in both SE and TP.

3.3 Dry deposition of N_r species

The annual dry deposition fluxes of NH_3, NO_2, HNO_3, pNH_4^+ and pNO_3^- were in the ranges of 0.5–15.2, 0.1–9.2, 0.2–10.0, 0.1–11.7 and 0.1–4.5 kg N ha^{-1} yr^{-1}, and averaged 7.7, 3.1, 3.7, 3.2 and 1.4 kg N ha^{-1} yr^{-1}, respectively (Fig. 4a). Comparing individual fluxes by region (Table 1), NC showed higher deposition levels for gaseous and particulate species. The deposition fluxes of gaseous species followed NC > SW > NE > SE > NW > TP for NH_3, NC > SW > SE > NE ≈ TP > NW for NO_2, and NC > SE > SW > NE > NW for NHO_3, while those of pNH_4^+ and pNO_3^- were NC > SW > SE > NE > NW > TP and NC > SW > SE ≈ TP > NW > NE, respectively. The

ACPD
15, 18365–18405, 2015

total dry N deposition across all sites ranged from 1.0 to 44.1 kg N ha^{-1} yr^{-1} (averaged 18.5 kg N ha^{-1} yr^{-1}). Gaseous N species were the primary contributors to total dry-deposited N in all six regions, ranging from 71 % (NC) to 81 % (NW), regardless of the missing HNO_3 data at a few sites. In general, NH_3 was predominant N_r species in total dry N deposition and accounted for 26–73 %, compared with 1–43 % from NO_2 and 8–29 % from HNO_3. When assessed by region, the contributions of individual species to total dry deposition were 1.9–5.0 times higher for NH_3 than NO_2. The average annual dry N deposition fluxes were 28.4, 18.5, 15.1, 12.2, 10.7 and 7.3 kg N ha^{-1} yr^{-1} in NC, SW, SE, NE, NW and TP, respectively (Table 1). By land use types, the annual mean dry N deposition followed the order of urban (24.2 kg N ha^{-1} yr^{-1}) > rural (20.7 kg N ha^{-1} yr^{-1}) > background (8.9 kg N ha^{-1} yr^{-1}). Also, there were clear differences in the dry deposition flux of each N_r species as well as in the total dry N deposition for the different land use types in the six regions (Fig. 3b).

3.4 Wet deposition of N_r species

Annual wet N deposition fluxes at the forty-three sites ranged from 1.0 to 19.1 kg N ha^{-1} yr^{-1} for NH_4^+-N and from 0.5 to 20.1 kg N ha^{-1} yr^{-1} for NO_3^--N (Fig. 4b). The annual wet deposition fluxes of NH_4^+-N were, on average, 1.3 times those of NO_3^--N. The total annual wet N (NH_4^+-N + NO_3^--N) deposition fluxes across all the sites were 1.5–32.5 kg N ha^{-1} yr^{-1} (average 19.3 kg N ha^{-1} yr^{-1}), with a large spatial variation. Region variation of annual wet N deposition followed the order of NC > SE > SW > NE > NW > TP for NH_4^+-N, and SE > NC > SW > NE > TP > NW for NO_3^--N, both of which differed from their orders of annual VWM concentration, reflecting differences in annual precipitation. Annual total wet N deposition fluxes averaged 24.6, 13.6, 7.4, 24.4, 17.6 and 7.6 kg N ha^{-1} yr^{-1}, respectively, in NC, NE, NW, SE, SW and TP.

ACPD
15, 18365–18405, 2015

3.5 Total annual dry and wet deposition of N_r species

The total (dry plus wet) annual N deposition at the 43 sites ranged from 2.9 to 75.2 kg N ha^{-1} yr^{-1} (average 37.8 kg N ha^{-1} yr^{-1}) for the period, with 22–82 % dry-deposited (Fig. S5). The contribution of reduced N deposition (NH_x, that is, wet NH_4^+-N deposition plus dry deposition of NH_3 and pNH_4^+) to the total N deposition (39–76 %) was, on average, 1.4 times greater than that of oxidized N deposition (NO_y; wet NO_3^--N deposition plus dry deposition of NO_2, HNO_3 and pNO_3^-). On a regional basis, the total deposition fluxes across the six regions were in the range of 14.9–53. kg N ha^{-1} yr^{-1}, with 54–66 % in the form of NH_x. The relative importance of dry vs. wet N deposition to the total deposition were different in the six regions, 54 vs. 46 % in NC, 49 vs. 51 % in NE, 59 vs. 41 % in NW, 38 vs. 62 % in SE, 52 vs. 48 % in SW, and 49 vs. 51 % in TP (Fig. 5).

Separated by land use types, total annual mean N deposition fluxes were 47.0, 42.0 and 24.7 kg N ha^{-1} yr^{-1} at the urban, rural and grassland sites, respectively, reflecting different anthropogenic impacts.

4 Discussion

4.1 Concentration of N_r species in air and precipitation

China is facing serious atmospheric N_r pollution induced by anthropogenic N_r emissions (Liu et al., 2011, 2013). The present study shows that monthly N_r concentrations of species, through comparisons among regions, have a distinct spatial variability with values significantly higher (all $p < 0.05$) in NC and significantly lower (all $p < 0.05$) in TP. Annual mean NH_3 and NO_2 concentrations at most sampling sites are in good agreement with the emission inventory and satellite observations by Gu et al. (2012), who reported NH_3 hotspots in the North China Plain and South Central China such as Jiangsu and Guangdong provinces, while NO_x hotspots were mainly in more devel-

ACPD
15, 18365–18405, 2015

oped regions such as the Jing-Jin-Ji (Beijing–Tianjin–Hebei), the Yangtze River Delta and the Pearl River Delta. Our results confirm that NC, which consumes large quantities of fertilizers (for food production) and fossil fuel (for energy supply) (Zhang et al., 2010) experiences the most serious N_r pollution in China; TP is the least polluted region due to much less human activity. When considering different land use types, the average total annual N_r concentrations ranked urban > rural > background, with significant differences (all $p < 0.05$) among them, despite site-to-site variability within regions. This reflects the dominant role of human activity on atmospheric N_r.

For individual N_r species, higher mean concentrations were observed at the urban sites than at rural and background sites (Fig. S3). Higher NH_3 concentration in urban areas may be associated with NH_3 emissions from biological sources, such as human, sewage disposal systems and refuse containers (Reche et al., 2002). In addition, NH_3 can be produced by over-reduction of NO in automobile catalytic converters (Behera et al., 2013), increasing ambient NH_3 concentrations in urban areas with high traffic densities. Between 2006 and 2013, the number of civil vehicles increased from 2.39 to 5.17 million in Beijing and from 0.46 to 1.72 million in Zhengzhou (NBSC, 2007–2014), which is likely to have resulted in elevated NH_3 emissions. Higher NO_2 concentrations are expected in urban areas due to NO_x emissions from the combustion of fossil fuels (Li and Lin, 2000), and also lead to higher HNO_3 concentrations in urban areas via NO_2 oxidation.

The higher pNH_4^+ and pNO_3^- concentrations observed at urban sites mainly resulted from the high concentrations at the northern urban sites (NC1~3, NW1 and NW2) (Figs. 2, S1c and d in Supplement). This is probably due to the fact that cities in northern China, such as Beijing and Zhengzhou in NC and Urumqi in NW, are being surrounded by intensive agricultural production. Rapid developments along with urbanization in suburban areas shorten the transport distance between NH_3 emitted from agriculture and SO_2 and NO_x emitted from fossil fuel combustion (Gu et al., 2014). This allows the pollutants to react more readily and form aerosols (e.g. $PM_{2.5}$), leading to high concentrations of pNH_4^+ and pNO_3^- near or within cities. This explanation is sup-

ACPD
15, 18365–18405, 2015

ported by the recent MEPC (2013) report that the annual average $PM_{2.5}$ concentrations in the cities of Beijing, Zhengzhou and Urumqi were more than twice the Chinese annual mean $PM_{2.5}$ standard value of 35 $\mu g\,m^{-3}$, whereas cities such as Guangzhou and Xining with little surrounding agricultural production had lower $PM_{2.5}$ concentrations. In China's 12th Five Year Plan (2011–2015), nationwide controls on NO_x emissions will be implemented along with controls on SO_2 and primary particle emissions (Wang et al., 2014). In order to better improve the regional air quality for metropolitan areas; our results suggest that strict control measures on both NH_3 and NO_x would be beneficial in NC, at least in the suburban areas.

Rural sites in this study also had relatively high concentrations of NO_2, HNO_3, pNH_4^+ and pNO_3^-, especially in northern China. This is mainly due to the combined effect of high NH_3 emissions from N fertilized farmland (Zhang et al., 2008a) and urban air pollution (e.g. NO_2, HNO_3, pNH_4^+ and pNO_3^-) transported from population centers to the surrounding rural areas (Luo et al., 2013). The lower air concentrations of N_r species at background sites can be ascribed to the lack of both substantial agricultural and industrial emissions. Additionally, higher wind speeds occurred at some background areas (e.g. NC12, NC13 and NW4) (Table S1 in the Supplement), favoring the dispersion of atmospheric pollutants.

We found that the VWM concentrations of NH_4^+-N and NO_3^--N were significantly higher (both $p < 0.05$) in northern China than in southern China and TP (Table 1), although the differences were not significant ($p > 0.05$) when comparing NE and NW with SW. This was due to multiple factors such as relative high N_r levels in northern China balanced by high rainfall in southern China (Figs. S2 and S6). However, regional variations in N_r concentrations in precipitation were not fully in accordance with ambient N_r concentrations (see Sect. 3.2). It is commonly accepted that N concentrations in precipitation are affected by the amount of precipitation (Yu et al., 2011). Negative correlations between precipitation amount and monthly volume-weighted concentrations of NH_4^+-N and NO_3^--N were obtained by fitting exponential models in all six regions (Fig. S7), indicating a dilution effect of rainwater on inorganic N concentration. The re-

ACPD
15, 18365–18405, 2015

lationships were not significant ($p > 0.05$) in NW and TP, which is probably caused by low precipitation amounts at or near the sampling sites. Nevertheless, dilution could explain some of the regional differences in precipitation N concentrations.

4.2 Dry and wet deposition of N_r species

A significant ($p < 0.001$) positive correlation was observed between annual dry N deposition and total annual concentrations of atmospheric N_r species across all sites (Fig. S8). Therefore, In NC higher concentrations of N_r species led to higher dry deposition rates. In TP, a remote region of China, atmospheric N_r concentrations were lower than those in the other five regions, and thus dry deposition was also lower than in the other regions. Among land use types the highest total N deposition was observed at urban sites, mainly attributable to elevated N_r emissions from urban sources (e.g., non-agricultural NH_3 emissions from landfills, wastewater treatments and NO_x emissions from traffic vehicles and power plants) and rapid development of intensive agricultural production in suburban areas surrounding cities. At the national scale, dry N deposition rates contributed almost half (22–82 %, averaging 48 %) of the total inorganic N deposition, indicating the importance of dry deposition monitoring for comprehensive N deposition quantification.

In this study, the regional variation of annual wet N deposition showed a different spatial pattern to that of annual mean total N_r concentrations in precipitation. These findings, together with no significant differences ($p > 0.05$) in total annual wet N deposition between NC and SE, reflect, not surprisingly, that regional wet N deposition is dependent not only on N_r concentrations in precipitation but also on annual rainfall amounts. As shown in Fig. 6, annual wet deposition fluxes of NH_4^+-N and NO_3^--N both showed significantly positive correlations with the corresponding annual VWM concentrations of inorganic N and annual precipitation amount, especially for NH_4^+-N, that more significant was found for precipitation amount than concentration (Fig. 6a and b). The measured wet N deposition rates (average 19.3 kg N ha^{-1} yr^{-1}) were almost twice the earlier average value of 9.9 kg N ha^{-1} yr^{-1} for period of 1990–2003 in

ACPD
15, 18365–18405, 2015

China (Lü and Tian, 2007). Our results show similar regional patterns and comparable magnitudes to those measured in the 2000s in China as reported by Jia et al. (2014) ($\sim 14\,kg\ N\ ha^{-1}\ yr^{-1}$) and Liu et al. (2013) ($\sim 21\,kg\ N\ ha^{-1}\ yr^{-1}$).

The NH_4^+-N/NO_3^--N ratio in wet deposition can be used to indicate the relative contribution of N_r from agricultural and industrial activities to N deposition (Fahey et al., 1999) because the major anthropogenic source of NH_4^+-N in precipitation is NH_3 volatilized from animal excrement and the application of nitrogenous fertilizers in agriculture, while anthropogenic sources of NO_3^--N in precipitation originate from NO_x emitted from fossil fuel combustion in transportation, power plant and factories (Cui et al., 2014). In this study the overall annual average ratio of NH_4^+-N/NO_3^--N in wet deposition was 1.3 ± 0.5 (standard deviation), slightly lower than average values of 1.6 in Europe (Holland et al., 2005) and 1.5 in the United States (Du et al., 2014), and similar to an average value (1.2) reported elsewhere for 2013 in China (Zhu et al., 2015). There was no significant difference (p =0.385) between annual mean ratios of NH_4^+-N/NO_3^--N among northern China, southern China and TP. Based on these findings, we conclude that NH_4^+-N from agricultural sources still dominates wet N deposition but the contribution has decreased drastically between the 1980s and the 2000s (Liu et al., 2013). Reduced N also contributed more than oxidized N to the total N deposition, and the ratio of reduced to oxidized N deposition overall averaged 1.7 in dry deposition and 1.4 in the total deposition (Figs. 4a and S5). For all Chinese regions except NC we cannot compare our data with other studies because observations for different pollution climate sites in other regions are lacking. For NC, the overall average total N deposition was 53.0 $\pm$ 13.6 $kg\ N\ ha^{-1}\ yr^{-1}$, 13–32 % lower than the previously estimated values in Northern China (Pan et al., 2012; Luo et al., 2013). This difference may reflect differences in the numbers of sampling sites, land use type and assumed dry deposition velocities. As expected, our estimated deposition was substantially higher than the results of Lü and Tian (2007), who suggested that the total N deposition ranged from 13 to 20 $kg\ N\ ha^{-1}\ yr^{-1}$ in NC. This is attributed to their omission of many major species (e.g., gaseous NH_3, HNO_3 and particulate N_r) from their data.

ACPD
15, 18365–18405, 2015

The overall mean annual deposition fluxes (wet plus dry) of NH_x and NO_y for the period 2010–2014 was graded into five levels and plotted on maps showing the spatial distribution of NH_3 and NO_x emissions (Fig. 7a and b). The anthropogenic emission data of NH_3 and NO_x for the year 2010 in China were obtained from the *GAINS* (*Greenhouse Gas and Air Pollution Interactions and Synergies*) model (http://www.iiasa.ac.at/), and emission details for the 33 provinces of China are summarized in Table S5. The spatial patterns of estimated NH_x and NO_y deposition compare reasonably well with the regional patterns of NH_3 and NO_x emissions, respectively, even though the emission data were estimated at the province scale. With emission data, N deposition can be used to distinguish regional differences in reactive N_r pollution. Across six regions, significantly positive correlations were found between NH_3 emissions and NH_x deposition fluxes ($R^2 = 0.883, p < 0.01$) (Fig. 7c), and between NO_x emissions and NO_y deposition fluxes ($R^2 = 0.796, p < 0.05$) (Fig. 7d), implying that the N deposition fluxes to the six regions are strongly dependent on the spatial pattern of anthropogenic N_r emissions among the regions. The slopes of the relationships of NH_x vs. NH_3, and NO_y vs. NO_x were 0.50 and 0.43, which could be roughly interpreted that NH_x and NO_y deposition fluxes represent about 50 % NH_3 and 43 % NO_x emissions, respectively.

Compared to dry and wet N deposition fluxes estimated by CASTNET in the United States, EMEP in Europe, and EANET sites in Japan, the average values of dry and wet deposition in China are much higher (Table 2). In China, the consumption rates of chemical fertilizer and fossil fuel have increased 2.0- and 3.2-fold, respectively, between the 1980s and the 2000s (Liu et al., 2013). As a result, the estimated total emission of NH_3 reached 9.8 Tg in 2006, contributing approximately 15 and 35 % to the global and Asian NH_3 emissions (Huang et al., 2012), and NO_x emissions from fossil fuel combustion increased from 1.1 Tg N in 1980 to about 6.0 Tg N in 2010 (Liu et al., 2013). The increasing NO_x and NH_3 emissions in China led to higher atmospheric N deposition than those observed in other regions.

ACPD
15, 18365–18405, 2015

According to Endo et al. (2011), the low dry deposition fluxes in CASTNET, EMEP and Japan's EANET network are due at least partly to low concentrations of N_r compounds and/or the omission of dry deposition fluxes of major N_r species (e.g., NO_2 and NH_3) from the data. Meanwhile, the low wet deposition fluxes at these networks are likely to be a result of the combined effects of low amounts of precipitation and, especially, low atmospheric N_r concentrations. In addition, emissions of nitrogen compounds in other parts of the world are declining. In the US, for example, NO_x emissions from the electric power industry and from vehicles were reduced from1990 to 2007 (and continue to decline), which explained the declined N deposition fluxes observed at CASTNET (MACTEC, 2008). In EMEP, the total NO_x emissions decreased from 2006 to 2007 in the 27 EMEP countries (Benedictow et al., 2009). N deposition has decreased or stabilized in the United States and Europe since the late 1980s or early 1990s with the implementation of stricter legislation to reduce emissions (Goulding et al., 1998; Holland et al., 2005). However, wet deposition of ammonia, which is not regulated, has increased in recent years in the US (Du et al., 2014).

4.3 Implications of monitoring N_r concentration and deposition on regional N deposition simulation

Our results show that atmospheric concentrations and deposition of N_r in China were high in the 2000s, although the government has made considerable efforts to control environmental pollution by improving air quality in mega cities during and after the 2008 Beijing Summer Olympic Games (Wang et al., 2010; Chan and Yao, 2008). Given the fact that the arithmetic averages used in this study cannot give a completely accurate evaluation of N_r levels for the regions of China due to the limited numbers of monitoring sites and ecosystem types, it is important to develop and improve the quantitative methods for determining N deposition across China.

Numerical models are very useful tools to quantify atmospheric N deposition (including both spatial and temporal variations), but a challenge to the modeling approaches is that observations to validate the simulated concentrations and deposition fluxes are

ACPD
15, 18365–18405, 2015

often lacking. In our study 43 monitoring sites were selected in a range of ecosystem types to provide more representative regional information on atmospheric N deposition in China. Although those measurements cannot define all aspects of N deposition across different regions, they add substantially to existing knowledge concerning the spatial patterns and magnitudes of atmospheric N deposition. The present measurements will be useful for better constraining emission inventories and evaluating simulations from atmospheric chemistry models. In future studies we will use models (e.g., FRAME, Dore et al., 2012) integrated with measurements from our monitoring network to fully address the spatial-temporal variations of atmospheric N deposition and its impacts on natural and semi-natural ecosystems at the regional/national level.

4.4 Uncertainty analysis of the N dry and wet deposition fluxes

The dry deposition fluxes were estimated by combining measured concentrations with modeled V_d. Thus, some uncertainties may arise in the inputs for dry deposition modeling. For example, underlying surface parameters (e.g., surface roughness length and land type) strongly affect dry deposition through their effect on both deposition velocity and the absorbability of the ground surface to each of the gaseous and particulate N_r species (Loubet et al., 2008). Dry deposition velocities of N_r in this study were only modeled for 2012 (The production of GEOS-5 meteorological data ended in May 2013). We used monthly mean V_d values for 2012 for corresponding months in other years at each site. This may also lead to uncertainty in our dry deposition estimation while small differences in monthly dry deposition velocities of N_r between different years were reported at ten sites (~ 1 %) in the northern China (Pan et al., 2012) and at a forest site (~ 11 %) in southern China (Fan et al., 2009). In addition, there is uncertainty in the deposition fluxes for both pNH_4^+ and pNO_3^- in our network, resulting from the difference between the cut-off sizes of particles in the samplers and that defined in the modeled V_d which were calculated for atmospheric $PM_{2.5}$ in GEOS-Chem model. For example, the cut-off sizes of the samples can collect also coarse NO_3^- particles (e.g. calcium nitrate) but should have little effect on NH_4^+ particles (mainly in the fine scale < 1 µm)

ACPD
15, 18365–18405, 2015

(Tang et al., 2009), resulting in an underestimation of pNO_3^- deposition. Furthermore, NH_3 fluxes over vegetated land are bi-directional and the net direction of this flux is often uncertain. A so-called canopy compensation point was used in previous studies (Sutton et al., 1998) to determine the direction of the NH_3 flux. Since the principle of bi-directional NH_3 exchange was not considered in this study, NH_3 deposition may be overestimated at rural sites with relatively high canopy compensation points (e.g. up to 5 µg N m^{-3}) due to fertilized croplands or vegetation (Sutton et al., 1993). Although we have improved the estimation of dry deposition greatly compared with previous work (e.g., Shen et al., 2009; Luo et al., 2013), further work is still required to increase the reliability and accuracy of N dry deposition values.

Since wet deposition was measured directly, the reported fluxes are considered more accurate than dry deposition fluxes but still some uncertainties exist. On one hand, the estimated fluxes obtained from the open precipitation samplers contain contributions from wet plus unquantifiable dry deposition (including both gases and particles) and therefore likely overestimate actual wet deposition (Cape et al., 2009). For example, our previous research showed that annual unquantifiable dry deposition (the difference between bulk and wet deposition, approx. 6 kg N ha^{-1} on average) accounted for 20 % of bulk N deposition based on observations at three rural sites on the North China Plain (Zhang et al., 2008b). This contribution increased to 39 % in urban areas based on a recent measurement (Zhang et al., 2015). On the other hand, dissolved organic N compounds, which have been observed to contribute to be around 25–30 % of the total dissolved nitrogen in wet deposition around the world (Jickells et al., 2013) and approximately 28 % of the total atmosphere bulk N deposition in China (Zhang et al., 2012b), were not considered in the present study. Their exclusion here would contribute to an underestimation of the total wet N deposition.

ACPD
15, 18365–18405, 2015

5 Conclusions

Our study represents the first effort to investigate inorganic dry and wet N deposition simultaneously, based on a nationwide monitoring network in China. We consider this unique dataset important not only for informing policy-makers about the abatement of pollutant emissions and ecosystem protection but also to validate model estimations of N deposition at the regional/national scale in China. The major results and conclusions are as follows.

1. Distinct spatial variability in annual mean concentrations of N_r species was observed, with regional averaged total N_r concentrations following the order of NC > NW ≈ SW > SE > NE > TP. The order of total concentrations of N_r species, based on land use type, was urban > rural > background.

2. Large spatial variations were observed for both dry and wet N deposition. The spatial pattern of dry deposition followed NC > SW > SE > NE > NW > TP, whereas the pattern was NC > SE > SW > NE > TP > NW for wet N deposition. Dry N deposition correlated well with total concentrations of N_r in the air, but differences were found between patterns of wet N deposition and the N_r concentration in precipitation. This reflects the dependence of regional wet N deposition on both N_r concentration and precipitation amounts.

3. Total annual N regional deposition fluxes followed NC > SE > SW > NE > NW > TP, which compared well with the spatial pattern of nitrogen emissions at the regional level. When considering land use type, the total N deposition was highest at urban sites, followed by rural sites and background sites, mainly attributable to N_r emissions from urban sources and rapid development of intensive agricultural production in suburban areas.

4. Dry deposition fluxes of N_r species on average contributed 48 % of the total N deposition (37.8 kg N ha^{-1} yr^{-1}) across all sites, indicating the importance of dry

ACPD
15, 18365–18405, 2015

deposition monitoring for a complete N deposition assessment at the national scale.

5. Annual average ratios of reduced N/oxidized N in dry and wet deposition were respectively 1.7 and 1.3, and 1.4 for the total deposition. It shows that reduced N, mainly from agricultural sources, still dominates dry, wet, and total N deposition in China.

The Supplement related to this article is available online at doi:10.5194/acpd-15-18365-2015-supplement.

Acknowledgements. This study was supported by the Chinese National Basic Research Program (2014CB954202), the China Funds for Distinguished Young Scholars of NSFC (40425007), and the National Natural Science Foundation of China (31121062, 41321064 and 41405144). The authors thank all technicians at monitoring sites in NNDMN.

References

Bey, I., Jacob, D. J., Yantosca, R. M., Logan, J. A., Field, B. D., Fiore, A. M., Li, Q., Liu, H., Mickley, L. J., and Schultz, M. G.: Global modeling of tropospheric chemistry with assimilated meteorology: model description and evaluation, J. Geophys. Res., 106, 23073–23096, 2001.

Behera, S. N., Sharma, M., Aneja, V. P., and Balasubramanian, R.: Ammonia in the atmosphere: a review on emission sources, atmospheric chemistry and deposition on terrestrial bodies, Environ. Sci. Pollut. R., 20, 8092–8131, doi:10.1007/s11356-013-2051-9, 2013.

Benedictow, A., Fagerli, H., Gauss, M., Jan, E., Tsyro, S., Nyıri, A., Simpson, D., Steensen, B. M., Klein, H., Valdebenito, A., Wind, P., Kirkevag, A., Griesfeller, J., Bartnicki, J., Olivie, D., Grini, A., Iversen, T., Semeena, V. S., Fagerli, H., Aas, W., Hjellbrekke, A. G., Mareckova, K., Wankmuller, R., Schneider, P., Solberg, S., Svendby, T., Liu, L., Posh, M., Vieno, M., Reis, S., Kryza, M., Werner, M., and Walaszek, K.: Transboundary acidification, eutrophication and ground level ozone in Europe in 2007, EMEP Report 1/2009, The Norwegian Meteorological Institute, Oslo, Norway, 19–28, 2009.

ACPD
15, 18365–18405, 2015

Cape, J. N., Van Dijk, N., and Tang, Y. S.: Measurement of dry deposition to bulk collectors using a novel flushing sampler, J. Environ. Monitor, 11, 353–358, doi:10.1039/B813812E, 2009.
Chan, C. K. and Yao, X. H.: Air pollution in mega cities in China, Atmos. Environ., 42, 1–42, doi:10.1016/j.atmosenv.2007.09.003, 2008.
Chen, D., Wang, Y., McElroy, M. B., He, K., Yantosca, R. M., and Le Sager, P.: Regional CO pollution and export in China simulated by the high-resolution nested-grid GEOS-Chem model, Atmos. Chem. Phys., 9, 3825–3839, doi:10.5194/acp-9-3825-2009, 2009.
Chen, X. Y. and Mulder, J.: Atmospheric deposition of nitrogen at five subtropical forested sites in South China, Sci. Total Environ., 378, 317–330, doi:10.1016/j.scitotenv.2007.02.028, 2007.
Clark, C. M. and Tilman, D.: Loss of plant species after chronic low-level nitrogen deposition to prairie grasslands, Nature, 451, 712–715, doi:10.1038/nature06503, 2008.
Cui, J., Zhou, J., Peng, Y., He, Y. Q., Yang, H., Mao, J. D., Zhang, M. L., Wang, Y. H., and Wang, S. W.: Atmospheric wet deposition of nitrogen and sulfur in the agroecosystem in developing and developed areas of Southeastern China, Atmos. Environ., 89, 102–108, doi:10.1016/j.atmosenv.2014.02.007, 2014.
Dentener, F., Drevet, J., Lamarque, J. F., Bey, L., Eickhout, B., Fiore, A. M. Hauglustaine, D., Horowitz, L. W., Krol, M., and Kulshrestha, U. C .: Nitrogen and sulfur deposition on regional and global scales: a multimodel evaluation, Global Biogeochem. Cy., 20, GB4003, doi:10.1029/2005GB002672, 2006.
Dore, A. J., Kryza, M., Hall, J. R., Hallsworth, S., Keller, V. J. D., Vieno, M., and Sutton, M. A.: The influence of model grid resolution on estimation of national scale nitrogen deposition and exceedance of critical loads, Biogeosciences, 9, 1597–1609, doi:10.5194/bg-9-1597-2012, 2012.
Du, E. Z., Vries, W. D., Galloway, J. N., Hu, X. Y., and Fang, J. Y.: Changes in wet nitrogen deposition in the United States between 1985 and 2012, Environ. Res. Lett., 9, 095004, doi:10.1088/1748-9326/9/9/095004, 2014.
EEA: Air Quality in Europe-2011 Report, Technical Report 12/2011, EEA, Kopenhagen, 2011.
Ellis, R. A., Jacob, D. J., Sulprizio, M. P., Zhang, L., Holmes, C. D., Schichtel, B. A., Blett, T., Porter, E., Pardo, L. H., and Lynch, J. A.: Present and future nitrogen deposition to national parks in the United States: critical load exceedances, Atmos. Chem. Phys., 13, 9083–9095, doi:10.5194/acp-13-9083-2013, 2013.

ACPD
15, 18365–18405, 2015

Endo, T., Yagoh, H., Sato, K., Matsuda, K., Hayashi, K., Noguchi, I., and Sawada, K.: Regional characteristics of dry deposition of sulfur and nitrogen compounds at EANET sites in Japan from 2003 to 2008, Atmos. Environ., 45, 1259–1267,doi:10.1016/j.atmosenv.2010.12.003, 2010.

Erisman, J. W., Vermeulen, A., Hensen, A., Flechard, C., Dammgen, U., Fowler, D., Sutton, M., Grunhage, L., and Tuovinen, J. P.: Monitoring and modelling of biosphere/atmosphere exchange of gases and aerosols in Europe, Environ. Pollut., 133, 403–413, doi:10.1016/j.envpol.2004.07.004, 2005.

Fahey, T. J., Williams, C. J., Rooney-Varga, J. N., Cleveland, C. C., Postek, K. M., Smith, S. D., and Bouldin, D. R.: Nitrogen deposition in and around an intensive agricultural district in central New York, J. Environ. Qual., 28, 1585–1600, doi:10.2134/jeq1999.00472425002800050025x, 1999.

Fang, J. L., Hu, Z. Y., Wang, T. J., Zhou, J., Wu, C. Y. H., and Xia, X.: Atmospheric inorganic nitrogen deposition to a typical red soil forestland in southeastern China, Environ. Monit. Assess., 159, 241–253, doi:10.1007/s10661-008-0626-6, 2009.

Flechard, C. R., Nemitz, E., Smith, R. I., Fowler, D., Vermeulen, A. T., Bleeker, A., Erisman, J. W., Simpson, D., Zhang, L., Tang, Y. S., and Sutton, M. A.: Dry deposition of reactive nitrogen to European ecosystems: a comparison of inferential models across the NitroEurope network, Atmos. Chem. Phys., 11, 2703–2728, doi:10.5194/acp-11-2703-2011, 2011.

Fowler, D., Coyle, M., Skiba, U., Sutton, M. A., Cape, J. N., Reis, S., Sheppard, L. J., Jenkins, A., Grizzetti, B., Galloway, J. N., Vitousek, P., Leach, A., Bouwman, A. F., Butterbach-Bahl, K., Dentener, F., Stevenson, D., Amann, M., and Voss, M.: The global nitrogen cycle in the twenty-first century, Philos. T. Roy. Soc. B, 368, 20130164, doi:10.1098/rstb.2013.0164, 2013.

Galloway, J. N., Dentener, F. J., Capone, D. G., Boyer, E. W., Howarth, R. W., Seitzinger, S. P., Asner, G. P., Cleveland, C. C., Green, P. A., Holland, E. A., Karl, D. M., Michaels, A. F., Porter, J. H., Townsend, A. R., and Vorosmarty, C. J.: Nitrogen cycles: past, present, and future, Biogeochemistry, 70, 153–226, 2004.

Galloway, J. N., Townsend, A. R., Erisman, J. W., Bekunda, M., Cai, Z., Freney, J. R., Martinelli, L. A., Seitzinger, S. P., and Sutton, M. A.: Transformation of the nitrogen cycle: recent trends, questions, and potential solutions, Science, 320, 889–892, 2008.

ACPD
15, 18365–18405, 2015

Galloway, J. N., Leach, A. M., Bleeker, A., and Erisman, J. W.: A chronology of human understanding of the nitrogen cycle, Philos. T. Roy. Soc. B, 368, 20130120, doi:10.1098/rstb.2013.0120, 2013.

Goulding, K. W. T., Bailey, N. J., Bradbury, N. J., Hargreaves, P., Howe, M., Murphy, D. V., Poulton, P. R., and Willison, T. W.: Nitrogen deposition and its contribution to nitrogen cycling and associated soil processes, New Phytol., 139, 49–58, 1998.

Gu, B. J., Ge, Y., Ren, Y., Xu, B., Luo, W. D., Jiang, H., Gu, B. H., and Chang, J.: Atmospheric reactive nitrogen in China: sources, recent trends, and damage costs, Environ. Sci. Technol., 46, 9240–9247, doi:10.1021/es301446g, 2012.

Gu, B. J., Sutton, M. A., Chang, S. X., Ge, Y., and Jie, C.: Agricultural ammonia emissions contribute to China's urban air pollution, Front. Ecol. Environ., 12, 265–266, doi:10.1890/14.WB.007, 2014.

Holland, E. A., Braswell, B. H., Sulzman, J., and Lamarque, J. F.: Nitrogen deposition onto the United States and Western Europe: synthesis of observations and models, Ecol. Appl., 15, 38–57, 2005.

Hu, H., Yang, Q., Lu, X., Wang, W., Wang, S., and Fan, M.: Air pollution and control in different areas of China, Crit. Rev. Env. Sci. Tec., 40, 452–518, doi:10.1080/10643380802451946, 2010.

Huang, X., Song, Y., Li, M. M., Li, J. F., Huo, Q., Cai, X. H., Zhu, T., Hu, M., and Zhang, H. S.: A high-resolution ammonia emission inventory in China, Global Biogeochem. Cy., 26, GB1030, doi:10.1029/2011GB004161, 2012.

Huang, Y. L., Lu, X. X., and Chen, K.: Wet atmospheric deposition of nitrogen: 20 years measurement in Shenzhen City, China, Environ. Monit. Assess., 185, 113–122, doi:10.1007/s10661-012-2537-9, 2013.

Jia, Y. L., Yu, G. R., He, N. P., Zhan, X. Y., Fang, H. J., Sheng, W. P., Zuo, Y., Zhang, D. Y., and Wang, Q. F.: Spatial and decadal variations in inorganic nitrogen wet deposition in China induced by human activity, Sci. Rep., 4, 3763, doi:10.1038/srep03763, 2014.

Jickells, T., Baker, A. R., Cape, J. N., Cornell, S. E., and Nemitz, E.: The cycling of organic nitrogen through the atmosphere, Philos. T. Roy. Soc. B, 368, 20130115, doi:10.1098/rstb.2013.0115, 2013.

Li, Y. E. and Lin, E. D.: Emissions of N_2O, NH_3 and NO_x from fuel combustion, industrial processes and the agricultural sectors in China, Nutr. Cycl. Agroecosys., 57, 99–106, 2000.

ACPD
15, 18365–18405, 2015

Liu, X. J., Song, L., He, C. E., and Zhang, F. S.: Nitrogen deposition as an important nutrient from the environment and its impact on ecosystems in China, J. Arid Land, 2, 137–143, 2010.

Liu, X. J., Duan, L., Mo, J. M., Du, E., Shen, J. L., Lu, X. K., Zhang, Y., Zhou, X. B., He, C. E., and Zhang, F. S.: Nitrogen deposition and its ecological impact in China: an overview, Environ. Pollut., 159, 2251–2264, doi:10.1016/j.envpol.2010.08.002, 2011.

Liu, X. J., Zhang, Y., Han, W. X., Tang, A., Shen, J. L., Cui, Z. L., Vitousek, P., Erisman, J. W., Goulding, K., Christie, P., Fangmeier, A., and Zhang, F. S.: Enhanced nitrogen deposition over China, Nature, 494, 459–462, doi:10.1038/nature11917, 2013.

Liu, X. J., Xu, W., Pan, Y. P., and Du, E. Z.: Liu et al. suspect that Zhu et al. (2015) may have underestimated dissolved organic nitrogen (N) but overestimated total particulate N in wet deposition in China, Sci. Total Environ., 520, 300–301, doi:10.1016/j.scitotenv.2015.03.004, 2015.

Loubet, B., Asman, W. A. H., Theobald, M. R., Hertel, O., Tang, S. Y., Robin, P., Hassouna, M., Dämmgen, U., Genermont, S., Cellier, P., and Sutton, M. A.: Ammonia deposition near hot spots: processes, models and monitoring methods, in: Atmospheric Ammonia: Detecting Emission Changes and Environmental Impacts, edited by: Sutton, M. A., Reis, S., Baker, S. M. H., Springer, Netherlands, 205–251, 2008.

Lü, C. Q. and Tian, H. Q.: Spatial and temporal patterns of nitrogen deposition in China: synthesis of observational data, J. Geophys. Res., 112, D22S05, doi:10.1029/2006JD007990, 2007.

Lü, C. Q. and Tian, H. Q.: Half-century nitrogen deposition increase across China: a gridded time-series data set for regional environmental assessments, Atmos. Environ., 97, 68–74, 2014.

Luo, X. S., Liu, P., Tang, A. H., Liu, J. Y., Zong, X. Y., Zhang, Q., Kou, C. L., Zhang, L. J., Fowler, D., Fangmeier, A., Christie, P., Zhang, F. S., and Liu, X. J.: An evaluation of atmospheric N_r pollution and deposition in North China after the Beijing Olympics, Atmos. Environ., 74, 209–216, doi:10.1016/j.atmosenv.2013.03.054, 2013.

MACTEC Engineering and Consulting, Inc. (MACTEC): Clean Air Status and Trends Network (CASTNET) 2007, Annual Report, U. S. Environmental Protection Agency, Washington, D.C., 5–30, 2008.

Maston, P., Lohse, K. A., and Hall, S. J.: The globalization of nitrogen deposition: consequences for terrestrial ecosystems, Ambio, 31, 113–119, 2002.

ACPD
15, 18365–18405, 2015

MEPC (Ministry of Environmental Protection of the People's Republic of China): China's environment and data center, available at: www.zhb.gov.cn/, last access: 23 April 2014.
NBSC (National Bureau of Statistics of China): China Statistical Yearbook 2007–2014, China Statistics Press, Beijing, available at: http://www.stats.gov.cn, 2007–2014.
Pan, Y. P., Wang, Y. S., Tang, G. Q., and Wu, D.: Wet and dry deposition of atmospheric nitrogen at ten sites in Northern China, Atmos. Chem. Phys., 12, 6515–6535, doi:10.5194/acp-12-6515-2012, 2012.
Reche, C., Viana, M., Pandolfi, M., Alastuey, A., Moreno, T., Amato, F., Ripoll, A., and Querol, X.: Urban NH_3 levels and sources in a Mediterranean environment, Atmos. Environ., 57, 153–164, doi:10.1016/j.atmosenv.2012.04.021, 2012.
Richter, A., Burrows, J. P., Nüß, H., Granier, C., and Niemeier, U.: Increase in tropospheric nitrogen dioxide over China observed from space, Nature, 437, 129–132, 2005.
Seinfeld, J. and Pandis, S.: Atmospheric Chemistry and Physics: From Air Pollution to Climate Change, 2nd edition, John Wiley and Sons, 1203 pp., 2006.
Schwede, D., Zhang, L., Vet, R., and Lear, G.: An intercomparison of the deposition models used in the CASTNET and CAPMoN networks, Atmos. Environ., 45, 1337–1346, doi:10.1016/j.atmosenv.2010.11.050, 2011.
Shen, J. L., Tang, A. H., Liu, X. J., Fangmeier, A., Goulding, K. T. W., and Zhang, F. S.: High concentrations and dry deposition of reactive nitrogen species at two sites in the North China Plain, Environ. Pollut., 157, 3106–3113, doi:10.1016/j.envpol.2009.05.016, 2009.
Simpson, D., Fagerli, H., Jonson, J. E., Tsyro, S., Wind, P., and Tuovinen, J. P.: Trans-boundary acidification and eutrophication and ground level ozone in Europe: unified EMEP model description, EMEP Status Report 1/2003 Part I, EMEP/MSC-W Report, The Norwegian Meteorological Institute, Oslo, Norway, 2003.
Skeffington, R. A. and Hill, T. J.: The effects of a changing pollution climate on throughfall deposition and cycling in a forested area in southern England, Sci. Total Environ., 434, 28–38, doi:10.1016/j.scitotenv.2011.12.038, 2012.
Sutton, M. A., Pitcairn, C. E. R., and Fowler, D.: The exchange of ammonia between the atmosphere and plant communities, Adv. Ecol. Res., 24, 301–393, doi:10.1016/S0065-2504(08)60045-8, 1993.
Sutton, M. A., Burkhardt, J. K., Guerin, D., Nemitz, E., and Fowler, D.: Development of resistance models to describe measurements of bi-directional ammonia surface–atmosphere exchange, Atmos. Environ., 32, 473–480, doi:10.1016/S1352-2310(97)00164-7, 1998.

ACPD
15, 18365–18405, 2015

Sutton, M. A., Tang, Y. S., Miners, B., and Fowler, D.: A new diffusion denuder system for long-term, regional monitoring of atmospheric ammonia and ammonium, Water Air Soil Poll. Focus, 1, 145–156, 2001.

Tang, Y. S., Simmons, I., van Dijk, N., Di Marco, C., Nemitz, E., Dammgen, U., Gilke, K., Djuricic, V., Vidic, S., and Gliha, Z.: European scale application of atmospheric reactive nitrogen measurements in a low-cost approach to infer dry deposition fluxes, Agr. Ecosyst. Environ., 133, 183–195, doi:10.1016/j.agee.2009.04.027, 2009.

Vitousek, P. M., Aber, J. D., Howarth, R. W., Likens, G. E., Matson, P. A., Schindler, D. W., Schlesinger, W. H., and Tilman, D. G.: Human alteration of the global nitrogen cycle: sources and consequences, Ecol. Appl., 7, 737–750, 1997.

Wang, S. X., Xing, J., Zhao, B., Jang, C., and Hao, J. M.: Effectiveness of national air pollution control policies on the air quality in metropolitan areas of China, J. Environ. Sci., 26, 13–22, doi:10.1016/S1001-0742(13)60381-2, 2014.

Wang, T., Nie, W., Gao, J., Xue, L. K., Gao, X. M., Wang, X. F., Qiu, J., Poon, C. N., Meinardi, S., Blake, D., Wang, S. L., Ding, A. J., Chai, F. H., Zhang, Q. Z., and Wang, W. X.: Air quality during the 2008 Beijing Olympics: secondary pollutants and regional impact, Atmos. Chem. Phys., 10, 7603–7615, doi:10.5194/acp-10-7603-2010, 2010.

Wesely, M. L.: Parameterization of surface resistances to gaseous dry deposition in regional-scale numerical-models, Atmos. Environ., 23, 1293–1304, 1989.

Yu, W. T., Jiang, C. M., Ma, Q., Xu, Y. G., Zou, H., and Zhang, S. C.: Observation of the nitrogen deposition in the lower Liaohe River Plain, Northeast China and assessing its ecological risk, Atmos. Res., 101, 460–468, doi:10.1016/j.atmosres.2011.04.011, 2011.

Zhang, F. S., Wang, J. Q., Zhang, W. F., Cui, Z. L., Ma, W. Q., Chen, X. P., and Jiang, R. F.: Nutrient use efficiency of major cereal crops in China and measures for improvement, Acta. Pedologia Sinica, 45, 915–924, 2008a (in Chinese).

Zhang, G. Z., Pan, Y. P., Tian, S. L., Cheng, M. T., Xie, Y. Z., Wang, H., and Wang, Y. S.: Limitations of passive sampling technique of rainfall chemistry and wet deposition flux characterization, Res. Environ. Sci., 28, 684–690, doi:10.13198/j.issn.1001-6929.2015.05.03, 2015.

Zhang, L., Jacob, D. J., Knipping, E. M., Kumar, N., Munger, J. W., Carouge, C. C., van Donkelaar, A., Wang, Y. X., and Chen, D.: Nitrogen deposition to the United States: distribution, sources, and processes, Atmos. Chem. Phys., 12, 4539–4554, doi:10.5194/acp-12-4539-2012, 2012a.

ACPD
15, 18365–18405, 2015

Zhang, Y., Liu, X. J., Fangmeier, A., Goulding, K. T. W., and Zhang, F. S.: Nitrogen inputs and isotopes in precipitation in the North China Plain, Atmos. Environ., 42, 1436–1448, doi:10.1016/j.atmosenv.2007.11.002, 2008b.

Zhang, Y., Dore, A. J., Ma, L., Liu, X. J., Ma, W. Q., Cape, J. N., and Zhang, F. S.: Agricultural ammonia emissions inventory and spatial distribution in the North China Plain, Environ. Pollut., 158, 490–501, doi:10.1016/j.envpol.2009.08.033, 2010.

Zhang, Y., Song, L., Liu, X. J., Li, W. Q., Lü, S. H., Zheng, L. X., Bai, Z. C., Cui, G. Y., and Zhang, F. S.: Atmospheric organic nitrogen deposition in China, Atmos. Environ., 46, 195–204, doi:10.1016/j.atmosenv.2011.09.080, 2012b.

Zhao, Y. H., Zhang, L., Pan, Y. P., Wang, Y. S., Paulot, F., and Henze, D. K.: Atmospheric nitrogen deposition to the northwestern Pacific: seasonal variation and source attribution, Atmos. Chem. Phys. Discuss., 15, 13657–13703, doi:10.5194/acpd-15-13657-2015, 2015.

Zhu, J. X., He, N. P., Wang, Q. F., Yan, G. F., Wen, D., Yu, G. R., and Jia, Y. L.: The composition, spatial patterns, and influencing factors of atmospheric wet nitrogen deposition in Chinese terrestrial ecosystems, Sci. Total Environ., 511, 777–785, doi:10.1016/j.scitotenv.2014.12.038, 2015.

ACPD
15, 18365–18405, 2015

Table 1. Concentrations of various N_r species and the estimated N deposition fluxes in the six regions of China. Data in parentheses are standard errors.

Region	Concentration ($\mu g\ N\ m^{-3}$)					Concentration ($mg\ N\ L^{-1}$)		Dry deposition ($kg\ N\ ha^{-1}\ yr^{-1}$)					Wet deposition ($kg\ N\ ha^{-1}\ yr^{-1}$)		DD[a]	WD	TD
	NH_3	NO_2	HNO_3	pNH_4^+	pNO_3^-	NH_4^+	NO_3^-	NH_3	NO_2	HNO_3	pNH_4^+	pNO_3^-	NH_4^+	NO_3^-			
NC	8.5	10.1	1.6	9.0	4.8	2.4	1.9	10.7	4.5	5.3	5.6	2.7	13.5	11.1	28.4	24.6	53.0
	(0.8)	(1.0)	(0.1)	(1.1)	(0.5)	(0.1)	(0.1)	(0.8)	(0.7)	(0.7)	(0.8)	(0.3)	(0.9)	(0.6)	(2.6)	(1.4)	(3.8)
NE	4.4	3.7	1.0	3.8	1.6	1.1	1.2	6.8	1.2	2.9	1.8	0.6	6.4	7.3	12.2	13.6	25.9
	(1.9)	(1.2)	(0.1)	(1.4)	(0.4)	(0.2)	(0.3)	(2.4)	(0.5)	(0.3)	(0.7)	(0.2)	(1.6)	(2.0)	(4.2)	(3.5)	(7.5)
NW	5.5	6.4	1.2	4.7	1.6	2.7	1.3	5.4	1.1	2.0	1.6	0.7	4.9	2.5	10.7	7.4	18.1
	(1.7)	(3.1)	(0.5)	(1.7)	(0.6)	(0.6)	(0.2)	(1.4)	(0.4)	(0.7)	(0.5)	(0.2)	(0.6)	(0.5)	(3.0)	(0.9)	(3.3)
SE	5.0	5.8	1.1	4.4	2.0	1.0	0.9	6.3	2.8	3.2	2.0	0.9	12.8	11.5	15.1	24.4	39.5
	(0.6)	(0.7)	(0.1)	(0.4)	(0.2)	(0.1)	(0.1)	(0.6)	(0.3)	(0.4)	(0.2)	(0.1)	(0.9)	(1.0)	(1.3)	(1.5)	(2.3)
SW	5.9	5.9	1.2	4.9	1.7	1.1	1.0	7.9	4.2	3.1	3.2	1.1	9.2	8.5	18.5	17.6	36.1
	(1.0)	(0.8)	(0.2)	(1.7)	(0.5)	(0.2)	(0.3)	(1.2)	(1.2)	(0.8)	(1.2)	(0.3)	(2.4)	(2.6)	(2.5)	(4.6)	(5.3)
TP	3.4	2.8	n.a.[b]	1.7	1.3	1.1	0.8	4.0	1.2	n.a.	1.3	0.9	4.5	3.1	7.3	7.6	14.9
	(2.3)	(2.4)		(1.5)	(1.0)	(0.9)	(0.6)	(3.0)	(1.0)		(1.2)	(0.8)	(3.5)	(2.6)	(6.0)	(6.1)	(12.1)
Average	6.1	6.8	1.3	5.7	2.7	1.6	1.3	7.7	3.1	3.7	3.2	1.4	10.4	9.0	18.5	19.3	37.8
	(0.9)	(1.0)	(0.2)	(0.9)	(0.4)	(0.2)	(0.2)	(1.2)	(0.5)	(0.6)	(0.5)	(0.2)	(1.6)	(1.4)	(2.8)	(2.9)	(5.8)

[a] DD: total dry N deposition, WD: total wet N deposition, TD: total N deposition.
[b] Not determined.

ACPD
15, 18365–18405, 2015

Table 2. Comparison of dry, wet, and total deposition fluxes of N_r compounds between NNDMN in China and 3 networks in other countries.

Network		Japan EANET network[a]			CASTNET[b]			EMEP[c,d]			NNDMN		
Number of sites or grids		10 sites			130 sites			2447 grids(0.5° × 0.5°)			43 sites		
Observation period		Apr 2003–Mar 2008			Apr 2006–Dec 2013			Jan 2003–Dec 2007			Aug 2006–Nov 2014		
N deposition ($kg\ N\ ha^{-1}\ yr^{-1}$)		Dry	Wet	Total	Dry	Wet	Total	Dry	Wet	Total	Dry	Wet	Total
	Average	3.9	6.6	10.6	3.1	1.3	4.4	3.9	4.8	8.7	18.5	19.3	37.8
	Median	4.1	5.9	11.2	3.0	0.7	4.1	3.7	4.7	8.5	17.0	21.6	36.4
	Max	7.0	15.8	18.2	9.7	10.3	19.6	15.8	16.9	28.0	44.1	32.5	75.2
	Min	1.0	2.1	3.0	0.03	0.1	0.3	0.1	0.6	0.7	1.0	1.5	2.9

[a] The Japan EANET data are sourced from Endo et al. (2011). Gaseous NO_2 was not included in estimates of dry N deposition.
[b] The CASNET data are available online (http://www.epa.gov/castnet/). Gaseous NH_3 was not included in estimates of dry N deposition.
[c] The EMEP data are sourced from Endo et al. (2011), in which the dry and wet deposition amounts at each grid covering 27 EMEP countries were estimated by the unified EMEP models (Simpson et al., 2003).

ACPD
15, 18365–18405, 2015

Figure 1. Geographical distribution of the forty-three monitoring sites in China.

ACPD
15, 18365–18405, 2015

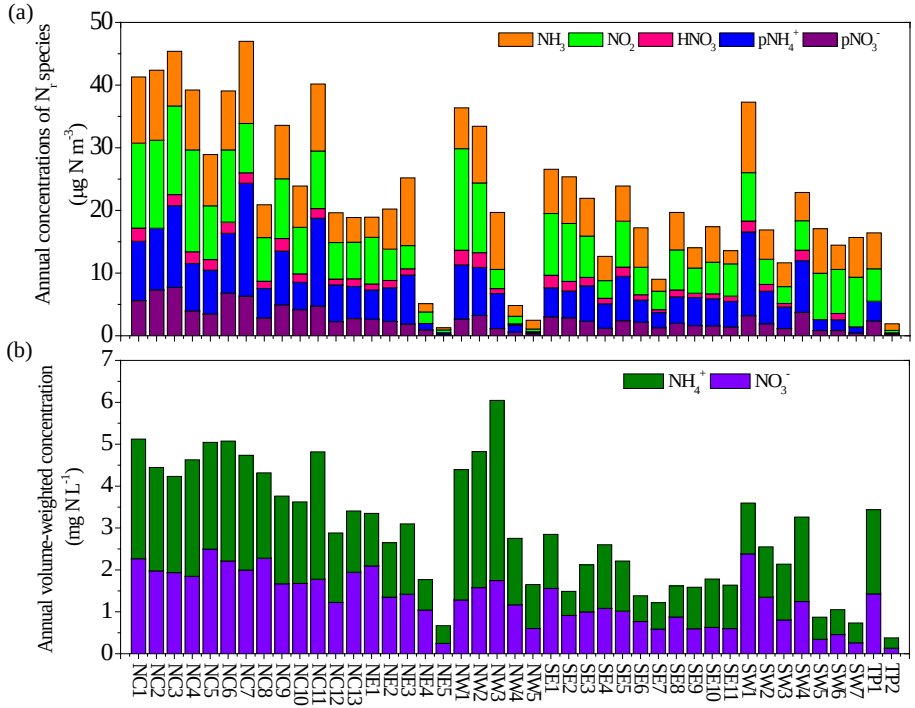

Figure 2. Annual mean concentrations of N_r compounds in air **(a)** and volume-weighted concentrations of inorganic nitrogen species in precipitation **(b)** at all monitoring sites.

ACPD
15, 18365–18405, 2015

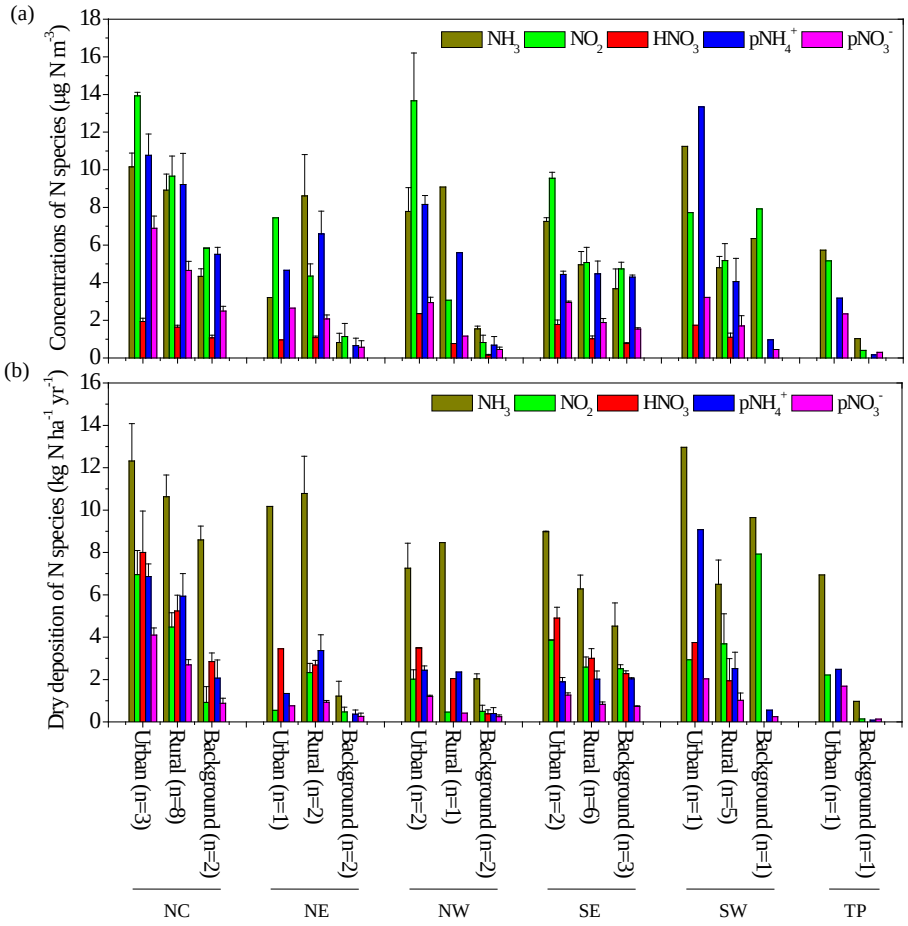

Figure 3. Atmospheric concentrations **(a)** and dry deposition fluxes **(b)** of N_r species at different land use types in the six regions of China. Error bars are standard errors of means. "*N*" in brackets denotes the number of sampling sites at each land use type.

ACPD
15, 18365–18405, 2015

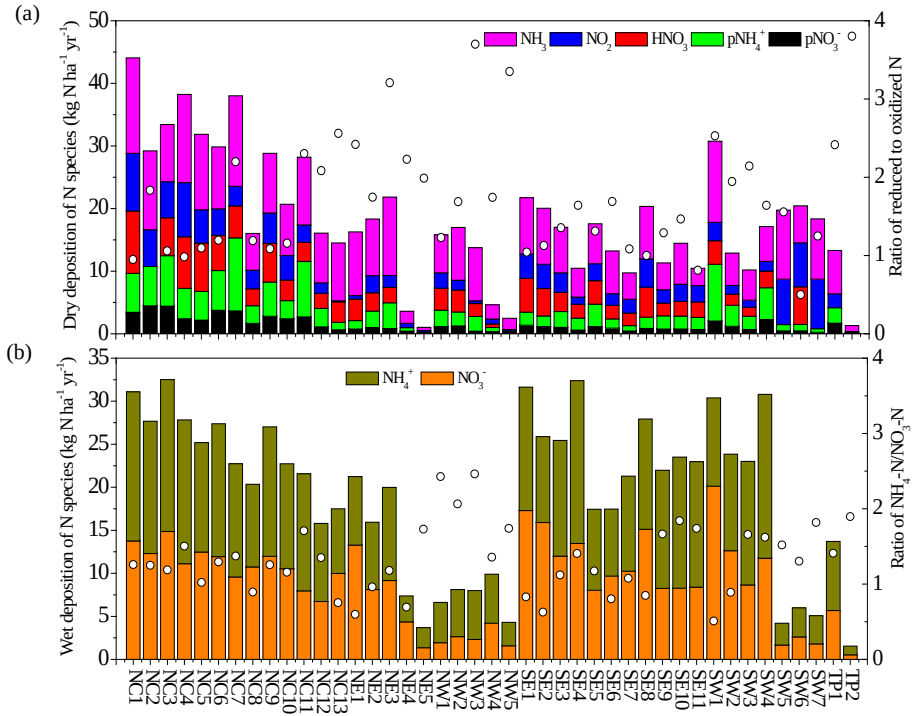

Figure 4. Annual deposition flux of various N_r species at the forty-three selected sites in China: **(a)** dry deposition flux; **(b)** wet deposition flux. Blank dots denote ratios of reduced N to oxidized N in dry deposition **(a)** and/or NH_4^+-N to NO_3^--N in wet deposition **(b)** at all sampling sites.

ACPD
15, 18365–18405, 2015

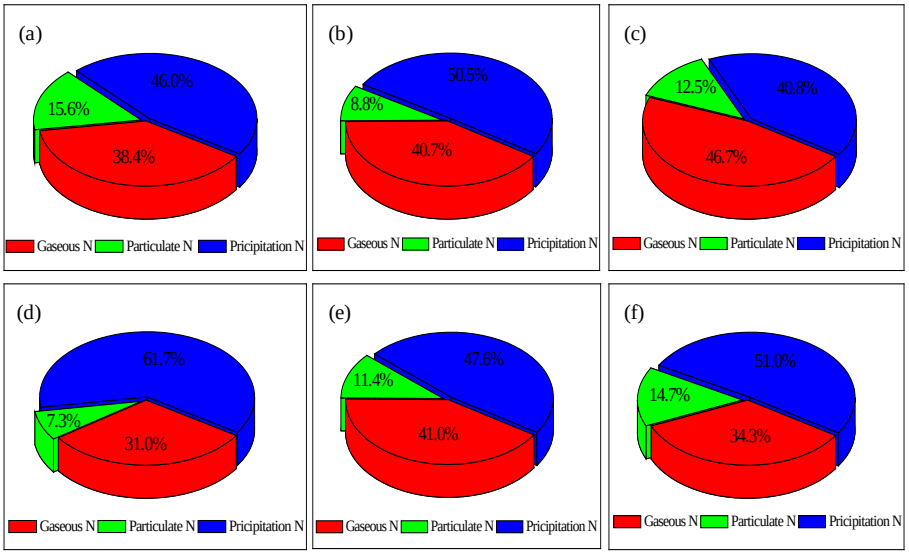

Figure 5. Contribution of different pathways (dry-deposited N = gaseous N + particulate N, wet-deposited N = precipitation N) to the estimated total N deposition in the six regions: **(a)** NC: north China; **(b)** NE: northeast China; **(c)** NW: northwest China; **(d)** SE: southeast China; **(e)** SW: southwest China; **(f)** TP: Tibetan Plateau.

ACPD
15, 18365–18405, 2015

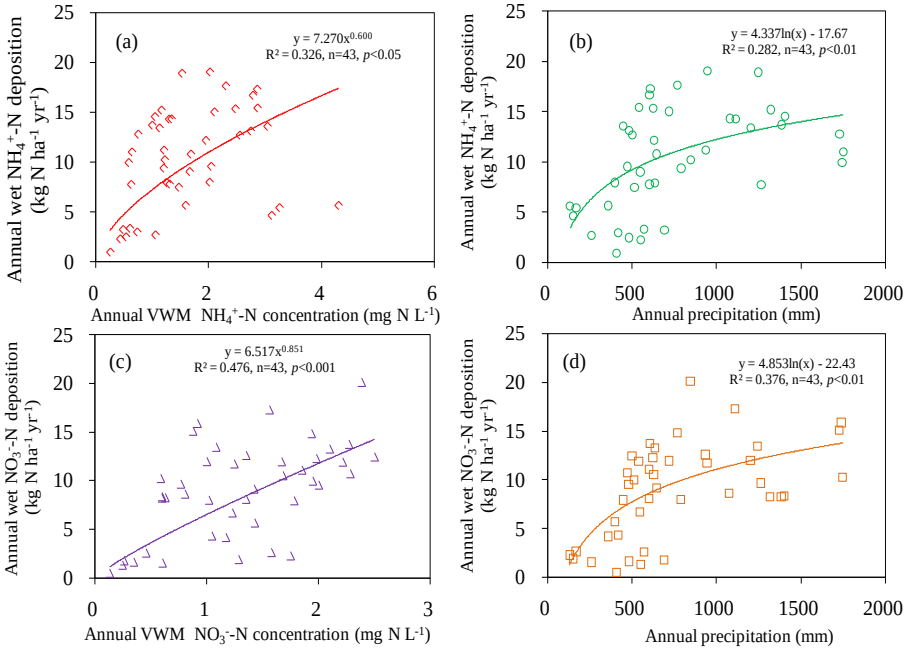

Figure 6. Correlations between annual wet NH_4^+-N deposition and annual volume-weighted concentration of NH_4^+-N **(a)** and annual precipitation **(b)**; between annual wet NO_3^--N deposition and annual volume-weighted concentration of NO_3^--N **(c)** and annual precipitation **(d)**.

ACPD
15, 18365–18405, 2015

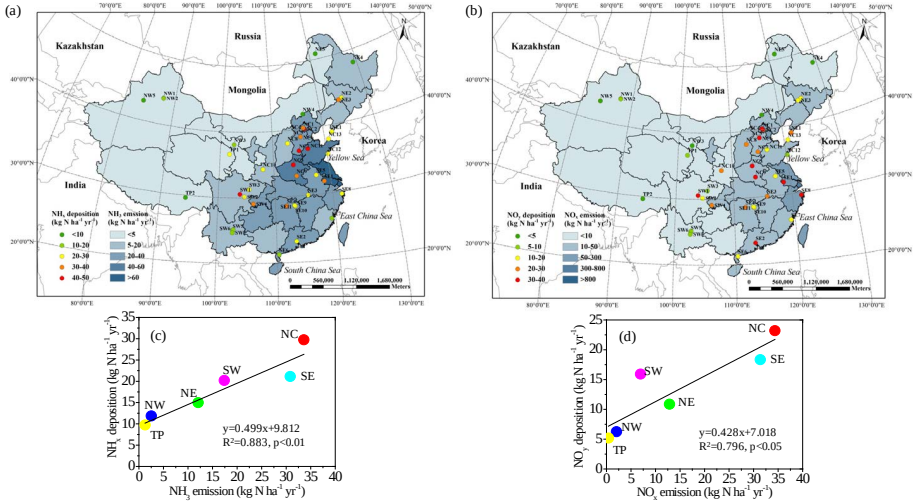

Figure 7. Spatial variation of atmospheric N deposition flux with emission distribution in China: **(a)** NH_3 emission vs. NH_x deposition; **(b)** NO_x emission vs. NO_y deposition; **(c)** relationship of NH_x deposition vs. NH_3 emission; **(d)** relationship of NO_y deposition vs. NO_x emission.

ACPD
15, 18365–18405, 2015